Hindawi Publishing Corporation
International Journal of Corrosion
Volume 2013, Article ID 543204, 13 pages
http://dx.doi.org/10.1155/2013/543204

Research Article

Corrosion Behavior and Adsorption Thermodynamics of Some Schiff Bases on Mild Steel Corrosion in Industrial Water Medium

S. S. Shivakumar and K. N. Mohana

Department of Chemistry, University of Mysore, Manasagangotri, Mysore 570006, India

Correspondence should be addressed to K. N. Mohana; drknmohana@gmail.com

Received 31 March 2013; Revised 2 August 2013; Accepted 3 August 2013

Academic Editor: Ramazan Solmaz

The inhibition performance and adsorption behavior of (E)-2-(3-nitrobenzylidene) hydrazine carbothioamide (SB_1) and (E)-2-(4-(dimethylamino) benzylidene) hydrazine carbothioamide (SB_2) on mild steel corrosion in industrial water medium have been investigated by gravimetric, potentiodynamic polarization and electrochemical impedance spectroscopy (EIS) techniques. The results revealed that inhibition efficiency depends on both the concentration of the inhibitors and temperature of the system. Increasing temperature reduces the inhibition efficiency of both inhibitors. Polarization studies indicated that these compounds behave as mixed type of inhibitors. The adsorption of both inhibitors was spontaneous and followed Langmuir adsorption isotherm. Thermodynamic parameters are calculated and discussed. The relation between inhibition efficiency and molecular structures of SB_1 and SB_2 was discussed by considering quantum chemical parameters. The surface adsorbed film was characterized by scanning electron microscopy (SEM).

1. Introduction

Mild steel (MS) is the widely used material in the fabrication of heating and cooling water system in many industries. Therefore, study of corrosion inhibition of mild steel in industrial water medium is a subject of technological importance. Organic compounds which are extensively used in several industries as corrosion inhibitors in various environments [1–3]. The anticorrosive property of these inhibitors depends on the specific interaction between certain functional groups in the inhibitors with the active centers on the metal surface [4–7]. Hetero atoms such as nitrogen, oxygen, and sulphur present in the inhibitors play an important role in this interaction by donating lone pair of electrons [8–12]. Hence the organic compounds containing these hetero atoms and multiple bonds behave as efficient corrosion inhibitors due to the availability of π-electrons for interaction with the metal surface [13]. The compounds containing an azo methine group (–C=N–) in their skeleton (Schiff bases) are the best examples for this type of corrosion inhibitors. They can be synthesized by condensation of primary amines with carbonyl compounds [14]. Schiff bases were reported as effective corrosion inhibitors for mild steel, copper, and aluminum in various media [15–24]. Although most of the commercial corrosion inhibitors are synthesized by using aldehydes and amines as main components, usually these Schiff bases possess more inhibition efficiency than their constituent carbonyls and amines [25, 26]. The higher inhibition efficiencies of Schiff bases are due to the presence of unoccupied π^*-orbital in the molecules. It supports electron back donation from the transition metal d-orbitals thus stabilizing the existing metal-inhibitor bond [27].

The present study focuses on the determination of anticorrosive property of SB_1 and SB_2 on mild steel in industrial water medium. Various thermodynamic functions of dissolution and adsorption process were evaluated. Further to understand the relationship between molecular structure of these substances and their inhibitive action, quantum chemical parameters such as the energy of the highest occupied molecular orbital (E_{HOMO}), the energy of

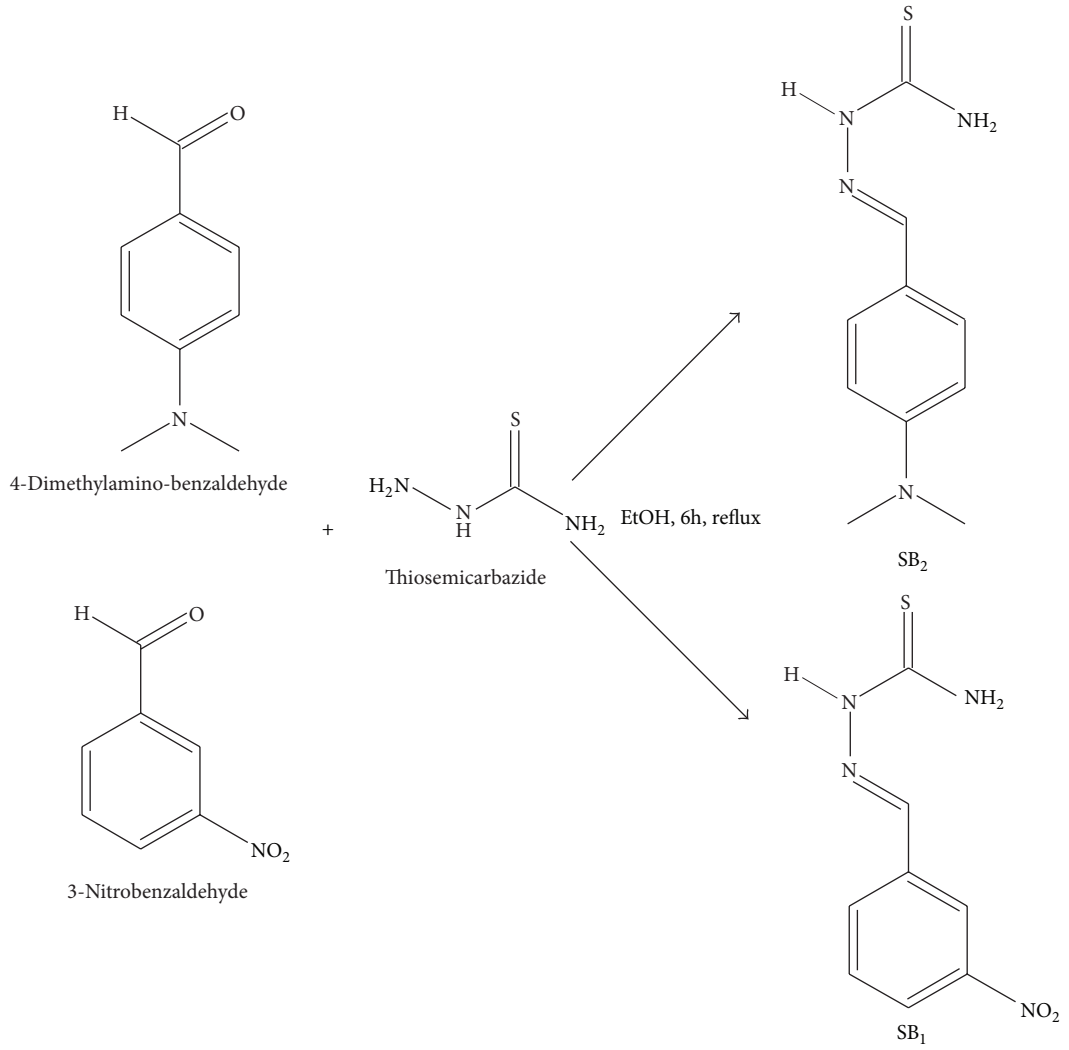

Figure 1: Synthesis of SB_1 and SB_2.

the lowest unoccupied molecular orbital (E_{LUMO}), the energy gap (ΔE), and the dipole moments (μ) have been computed and discussed.

2. Experimental

2.1. Materials. The Schiff bases, SB_1 and SB_2, were synthesized according to the literature method [28, 29]. The synthesis schemes of SB_1 and SB_2 are illustrated in Figure 1. Corrosion studies were performed on mild steel coupons with a dimension 2×2×0.1 cm. The chemical composition (wt%) of mild steel used for the experiment is 0.016 P, 0.322 Si, 0.01 Al, 0.062 Cr, 0.05 Mn, 0.09 C, 0.05 S and the remainder iron (Fe). Prior to each experiment, the surface of the specimen was polished under running tap water using emery paper of grade numbers, 220 to 1200, and rinsed with distilled water, dried on a clean tissue paper, immersed in benzene for five seconds, dried and immersed in acetone for five seconds, and dried with clean tissue paper. Finally, they are kept in a desiccator for one hour until use. The industrial water used throughout the experiment was taken from the sugar industries around Mysore city, India. The pH of the industrial water used was 5.45, and the chemical composition (mg L^{-1}) of industrial water was (ppm) 7500 Cl^-, 64 Ca^{2+}, 3440 SO_4^{2-}, 23 Mg^{2+}, 140 Na^+, and 0.28 PO_4^{3-}.

2.2. Weight Loss Method. In weight loss measurements, mild steel coupons were immersed in 200 mL of industrial water without and with various concentrations of the inhibitors. The metal specimens were removed from the test solutions after 10 hours at 30–60°C and the weight loss was determined using LP 120 digital balance with sensitivity of ±0.1 mg. The temperature of the medium was maintained using thermostatically controlled water bath (Weiber, India) under aerated condition. Weight loss values obtained were used for the calculation of corrosion rate in mg $cm^{-2}d^{-1}$.

2.3. Electrochemical Measurements. Polarization and EIS experiments were carried out using a CHI660D electrochemical workstation. A three-electrode cell configuration

consisting of rectangular mild steel specimen as working electrode (WE), a platinum electrode as counter (CE), and a saturated calomel electrode (SCE) as a reference was used. The specimen was pretreated similarly as done in the gravimetric measurements. All the experiments were carried out in industrial water medium at 30°C and at different concentrations of inhibitor. Potentiodynamic polarization measurements were performed in the potential range from −900 to +500 mV with a scan rate of 0.4 mV s^{-1} for an immersion period of 1 h. The AC impedance measurements were performed in the frequency range of 10 kHz to 0.05 Hz with signal amplitude of ±10 mV and EIS results were fitted by using CH Instruments Software version 12.04.

2.4. Quantum Chemical Calculations. The molecular structures of SB_1 and SB_2 were fully geometrically optimized by AM1 semiempirical method with Spartan' 08 V1.2.0. Four main related parameters such as the energy of the highest occupied molecular orbital (E_{HOMO}), the energy of the lowest unoccupied molecular orbital (E_{LUMO}), energy gap ($\Delta E = E_{LUMO} - E_{HOMO}$), and dipole moment ($\mu$) were gained. MOPAC calculations were carried out for four different Hamiltonians including parametric model 3 (PM3), Austin model 1 (AM1), Recif model 1 (RM1), and modified neglect of diatomic overlap model (MNDO). Mulliken charge population of atoms in the inhibitor was also calculated.

2.5. Scanning Electron Microscopy. The SEM analysis was performed using a JSM-5800 electron microscope with the working voltage of 20 kV and the working distance 24 mm. In SEM macrographs, the specimens were exposed to the industrial water in the absence and the presence of inhibitors under optimum conditions after 10 h of immersion. The SEM images were taken for pure mild steel and mild steel specimens immersed in industrial water without and with inhibitors.

3. Results and Discussion

3.1. Gravimetric Measurements. The weight loss of mild steel coupons in industrial water medium in the absence and presence of different concentrations of SB_1 and SB_2 was determined after 10 h of immersion period at 30–60°C. The percentage inhibition efficiency (IE %) and the degree of surface coverage (θ) were calculated and presented in Table 1. The corrosion rate (W) was computed using the following equation:

$$W = \frac{m_1 - m_2}{At}, \tag{1}$$

where m_1 and m_2 are the weight losses (mg) before and after immersion in the test solutions, A is the area of the specimen (cm^2), and t is the exposure time (day). The inhibition efficiency (IE%) was computed using the following equation:

$$\text{IE}\,\% = \frac{W_a - W_p}{W_a} \times 100, \tag{2}$$

where W_a and W_p are the corrosion rates in the absence and presence of the inhibitor, respectively. It can be observed from Table 1 that the inhibition efficiency increases with increase in the concentration of both SB_1 and SB_2. Maximum efficiencies (IE %) of SB_1 and SB_2 were achieved at 26.79×10^{-4} and 27.03×10^{-4} M concentrations, respectively. Further increase in the concentration did not cause any appreciable increase in the inhibition performance of the inhibitors. The parameter (θ), which represents the part of the metal surface covered by the inhibitor, molecules increases as the inhibitor concentration is increased. The increase in inhibition efficiencies with increasing concentration (Table 1) suggests that the SB_1 and SB_2 may be first adsorbed on the metal surface and cover some sites of the metal surface, then probably form monomolecular layers on which the insoluble products (by forming a complex) thereby protecting from corrosion [30].

3.2. Polarization Measurements. Polarization behavior of mild steel in industrial water without and with different concentration of SB_1 and SB_2 is shown in Figures 3(a) and 3(b), and various electrochemical parameters such as corrosion potential (E_{corr}), corrosion current density (I_{corr}), and percentage inhibition efficiency are obtained from the intersection of the anodic and cathodic Tafel lines of the polarization curve at E_{corr} and are given in Table 2. The IE% values were calculated from the following equation:

$$\text{IE}\,\% = \frac{(I_{corr})_a - (I_{corr})_p}{(I_{corr})_a} \times 100, \tag{3}$$

where $(I_{corr})_a$ and $(I_{corr})_p$ are the corrosion current density in the absence and presence of inhibitor, respectively.

It was observed that both cathodic and anodic curves show lower current density in presence of the inhibitors molecules. This indicates that SB_1 and SB_2 inhibit the corrosion process. The polarization measurements also clearly illustrate the fact that the inhibitor molecules under the studied conditions bring down the corrosion current density without causing any considerable change in the corrosion mechanism, suggesting that the addition of both SB_1 and SB_2 reduces anodic dissolution of iron and also retards hydrogen evolution reaction [31]. If the difference in E_{corr} values between inhibited and uninhibited solution is greater than 85 mV, a compound can be recognized as an anodic or a cathodic type inhibitor [32]. In the present study maximum displacement of the corrosion potentials (E_{corr}) was about −44 mV and −39 mV in the presence of SB_1 and SB_2, respectively. Thus both SB_1 and SB_2 act as mixed type of inhibitors.

3.3. EIS Measurements. Electrochemical impedance spectroscopy gives information about the kinetics of the electrode processes as well as the surface properties of the studied system. The shape of Nyquist plots gives mechanistic information. Figures 4(a) and 4(b) present the effect of inhibitor concentration on the impedance behavior of mild steel in industrial water medium at 30°C. It is apparent from Nyquist plots that the impedance response of mild steel in industrial

Table 1: W and IE % obtained from weight loss measurements of mild steel in industrial water containing various concentrations of SB_1 and SB_2 at different temperatures.

Temperature (°C)	SB_1			SB_2		
	C (mole)	W (mg/cm^{2}d)	IE %	C (mole)	W (mg/cm^{2}d)	IE %
30	Blank	2.029	—	Blank	2.029	—
	4.46×10^{-4}	1.231	39.32	4.51×10^{-4}	0.993	51.05
	8.93×10^{-4}	0.877	56.77	9.01×10^{-4}	0.749	63.08
	13.39×10^{-4}	0.694	65.79	13.51×10^{-4}	0.613	69.78
	17.86×10^{-4}	0.527	74.02	18.02×10^{-4}	0.525	74.12
	22.32×10^{-4}	0.421	79.25	22.52×10^{-4}	0.428	78.90
	26.79×10^{-4}	0.340	83.27	27.03×10^{-4}	0.401	80.23
40	Blank	3.103	—	Blank	3.103	—
	4.46×10^{-4}	0.81	73.89	4.51×10^{-4}	1.714	44.77
	8.93×10^{-4}	0.73	76.47	9.01×10^{-4}	1.281	58.72
	13.39×10^{-4}	0.61	80.34	13.51×10^{-4}	1.045	66.33
	17.86×10^{-4}	0.54	82.59	18.02×10^{-4}	0.939	69.73
	22.32×10^{-4}	0.43	86.14	22.52×10^{-4}	0.813	73.80
	26.79×10^{-4}	0.37	88.07	27.03×10^{-4}	0.722	76.73
50	Blank	4.644	—	Blank	4.644	—
	4.46×10^{-4}	1.26	72.86	4.51×10^{-4}	2.832	39.02
	8.93×10^{-4}	1.09	76.52	9.01×10^{-4}	2.213	52.35
	13.39×10^{-4}	0.90	80.62	13.51×10^{-4}	1.811	61.00
	17.86×10^{-4}	0.82	82.34	18.02×10^{-4}	1.541	66.82
	22.32×10^{-4}	0.69	85.14	22.52×10^{-4}	1.341	71.12
	26.79×10^{-4}	0.60	87.08	27.03×10^{-4}	1.164	74.94
60	Blank	7.202	—	Blank	7.202	—
	4.46×10^{-4}	1.79	46.56	4.51×10^{-4}	4.823	33.03
	8.93×10^{-4}	1.58	52.83	9.01×10^{-4}	3.891	45.97
	13.39×10^{-4}	1.36	59.40	13.51×10^{-4}	3.231	55.14
	17.86×10^{-4}	1.24	62.98	18.02×10^{-4}	2.992	58.46
	22.32×10^{-4}	1.09	67.46	22.52×10^{-4}	2.697	62.55
	26.79×10^{-4}	0.92	72.53	27.03×10^{-4}	2.247	68.80

Table 2: E_{corr}, I_{corr}, R_{ct} and IE (%) obtained from polarization and impedance measurements for mild steel in industrial water medium containing various concentrations of SB_1, and SB_2 at 30°C.

Inhibitor	C (M)	EIS			Polarization		
		R_{ct} (Ω cm^2)	C_{dl} (μF cm^{-2})	IE %	E_{corr} (mV)	I_{corr} (μA cm^{-2})	IE %
SB_1	Blank	251	189.2	—	−527	76.41	—
	4.46×10^{-4}	440	121.8	42.95	−499	42.32	44.61
	8.93×10^{-4}	653	82.1	61.56	−494	30.13	60.57
	13.39×10^{-4}	911	58.9	72.45	−488	21.54	71.81
	17.86×10^{-4}	1315	40.8	80.91	−480	15.64	79.53
	22.32×10^{-4}	1380	38.9	81.81	−482	13.79	81.95
	26.79×10^{-4}	1690	31.7	85.15	−483	10.24	86.60
SB_2	Blank	251	189.2	—	−527	76.41	—
	4.51×10^{-4}	501	107.2	49.90	−495	39.12	48.80
	9.01×10^{-4}	723	74.1	65.28	−490	29.44	61.47
	13.51×10^{-4}	958	55.9	73.80	−482	20.11	73.68
	18.02×10^{-4}	1183	45.3	78.78	−485	16.98	77.78
	22.52×10^{-4}	1314	40.8	80.90	−487	15.33	79.94
	27.03×10^{-4}	1438	37.3	82.55	−488	13.84	81.89

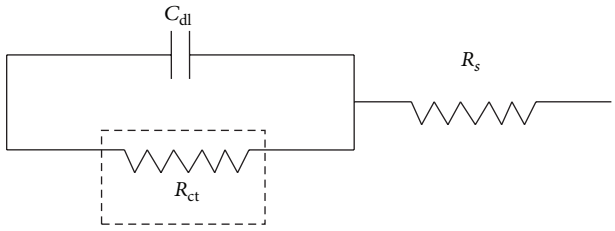

Figure 2: Equivalent circuit diagram.

water medium has significantly changed after the addition of the inhibitors. This shows that the impedance of the medium increased with increasing the concentration of both the inhibitors. The extracted impedance parameters from EIS plots are listed in Table 2.

The simple equivalent Randle circuit is shown in Figure 2 which includes the solution resistance (R_s), charge transfer resistance (R_{ct}), and double layer capacitance (C_{dl}). The inhibition efficiency IE (%) was calculated using the charge transfer resistance as follows:

$$\text{IE}\,\% = \frac{1/(R_{ct})_a - 1/(R_{ct})_p}{1/(R_{ct})_a} \times 100, \tag{4}$$

where $(R_{ct})_a$ and $(R_{ct})_p$ are charge transfer resistance of mild steel in the absence and presence of the inhibitor, respectively. From Table 2, it is clear that the data obtained from EIS are in close correlation with those obtained from weight loss and potentiodynamic polarization methods.

Inspection of Table 2 showed that increase in the concentration of the inhibitors increases the R_{ct} values and hence inhibition efficiency increases, indicating an insulated adsorption layer formation. The R_{ct} values calculated from EIS results represent the sum of the resistances of double layer region between the metal and the electrolyte solutions. The decrease in C_{dl} values is due to decrease in local dielectric constant and/or an increase in the thickness of the electrical double layer, indicating that both SB_1 and SB_2 act by adsorption at the mild steel/solution interface [33] and the decrease in C_{dl} values with an increase in the concentration of SB_1 and SB_2 was the result of an increase in the surface coverage by SB_1 and SB_2, which led to an increase in the inhibition efficiency. The thickness of the adsorbed layer δ_{org} is related to C_{dl} by the following equation [34]:

$$\partial_{org=\varepsilon_o\varepsilon_r/C_{dl}}, \tag{5}$$

where δ_0 and δ_r are the absolute and relative dielectric constant, respectively. The change in C_{dl} values was also caused by the gradual replacement of water molecules by the adsorption of the inhibitor molecules on the metal surface, and hence decreasing the extent of metal dissolution [33, 35].

3.4. Adsorption Studies. The study of adsorption isotherms gives an idea about the adsorptive behavior of the inhibitor molecule which can provide important information about the nature of the metal-inhibitor interaction. Organic inhibitors inhibit the corrosion by adsorption onto the metal surface. It depends on the nature as well as the surface charge of the metal, the adsorption mode, its chemical structure, and the type of the solution [36]. Two main types of interaction can describe the adsorption of the organic compounds are physical adsorption and chemical adsorption. These are influenced by the chemical structure of the inhibitor, the type of the electrolyte, and the charge and nature of the metal. The surface coverage, θ of the metal surface covered by the adsorbed inhibitor, was evaluated from weight loss measurements using the following equation:

$$\theta = 1 - \frac{W_a}{W_p}. \tag{6}$$

Several adsorption isotherms were tested to fit with the experimental data. These include the Langmuir, Frumkin, Temkin, Freundlich, and Flory-Huggins isotherms. The best fit was obtained from the Langmuir isotherm. The Langmuir isotherm equation is of the following form:

$$\frac{C}{\theta} = \frac{1}{K_{ads}} + c. \tag{7}$$

From (7) a plot of C/θ against C gives straight lines (Figures 5(a) and 5(b)) with slope around unity. The coefficient of correlation, R^2, gave the degree of fit between the experimental data and the isotherm equation. The equilibrium constant for the adsorption process (K_{ads}) is related to the standard Gibbs free energy of adsorption (ΔG_{ads}) by the following equation:

$$K_{ads} = \frac{1}{55.5} \exp\left(\frac{-\Delta G_{ads}}{RT}\right). \tag{8}$$

The negative ΔG_{ads} values (Table 3) are consistent with the spontaneity of the adsorption process and the stability of the adsorbed layer on the mild steel surface [37]. It has been reported [38] that the values of ΔG_{ads} up to -20 kJ mol^{-1} the adsorption was regarded as physisorption, the inhibition acts due to the electrostatic interaction between the charged molecules and the charged metal, while its values around -40 kJ mol^{-1} or smaller was considered as chemisorption, which is due to the charge sharing or a transfer from the inhibitor molecules to the metal surface to form covalent bond. The ΔG_{ads} values obtained in this study range from -28 to -32 kJ mol^{-1}. It suggested that the adsorption mechanism of investigated inhibitors on mild steel in industrial water is physisorption. The negative values of ΔH_{ads} mean that the dissolution process is an exothermic phenomenon [39]. The negative values of ΔS_{ads} imply that the activated complex in the rate determining step represents an association rather than a dissociation step, meaning that a decrease in disordering takes place on going from reactants to the activated complex [40].

3.5. Effect of Temperature. The effect of temperature (30–60°C) on the corrosion rate of mild steel in industrial water medium in the absence and presence of various concentrations of the inhibitors during 10 h of immersion was studied using gravimetric measurements (Table 1). The

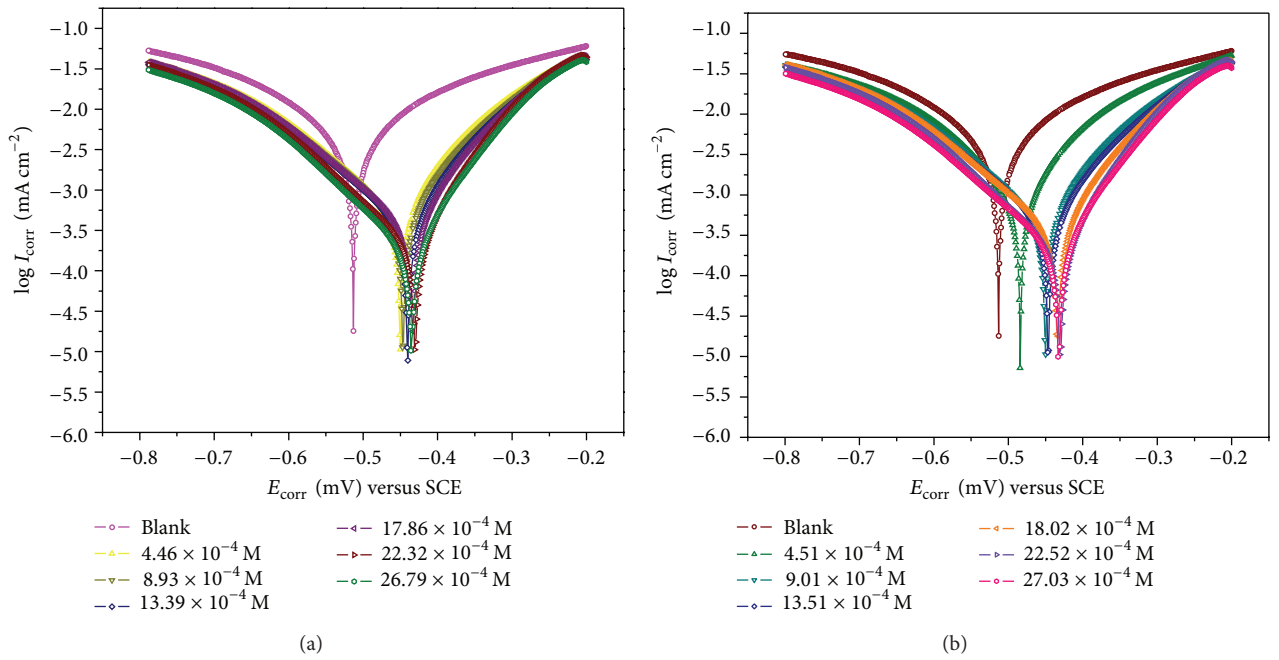

FIGURE 3: (a) Polarization curves for mild steel in industrial water containing different concentrations of SB_1 at 30°C. (b) Polarization curves for mild steel in industrial water containing different concentrations of SB_2 at 30°C.

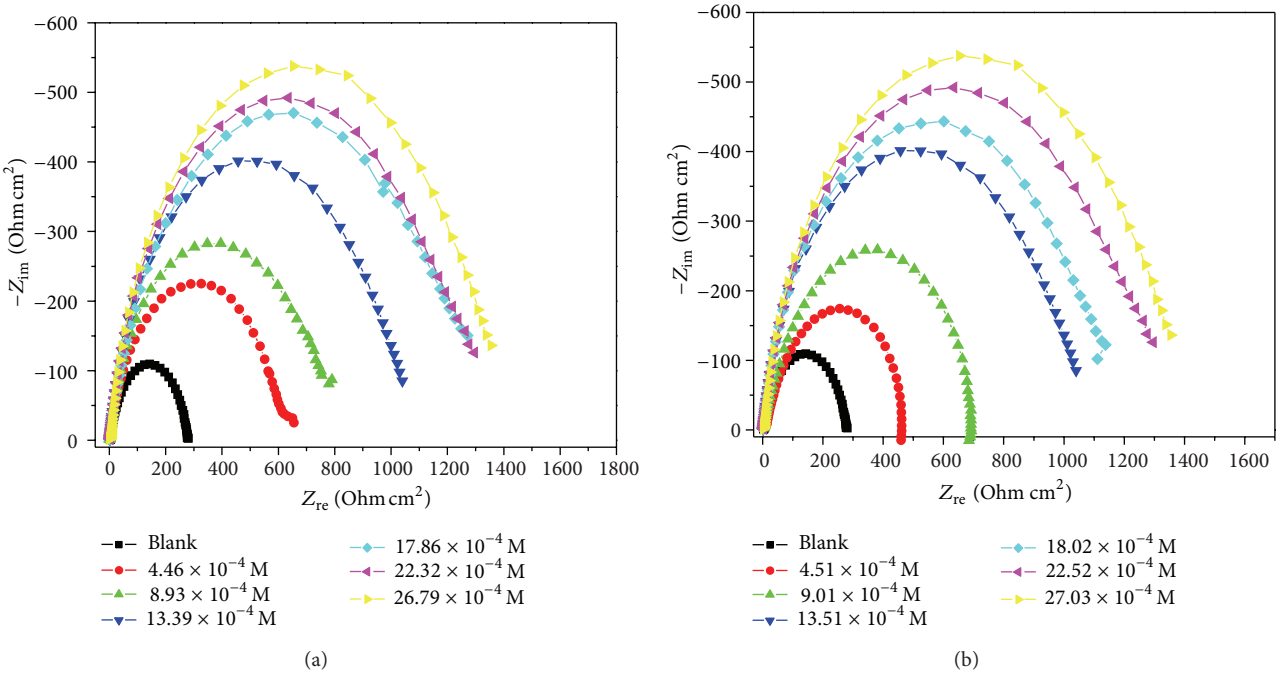

FIGURE 4: (a) Nyquist plots of mild steel in industrial water medium in the absence and presence of various concentrations of SB_1 at 30°C. (b) Nyquist plots of mild steel in industrial water medium in the absence and presence of various concentrations of SB_2 at 30°C.

results are presented in Table 4. From Table 1 it is clear that the w increases with increasing the temperature in the absence of the inhibitor. However, this increase seems slightly in presence of the inhibitors. The relationship between the corrosion rate (W) of mild steel and temperature (T) can be expressed by the Arrhenius equation:

$$W = k \exp \frac{-E_a^*}{RT}, \tag{9}$$

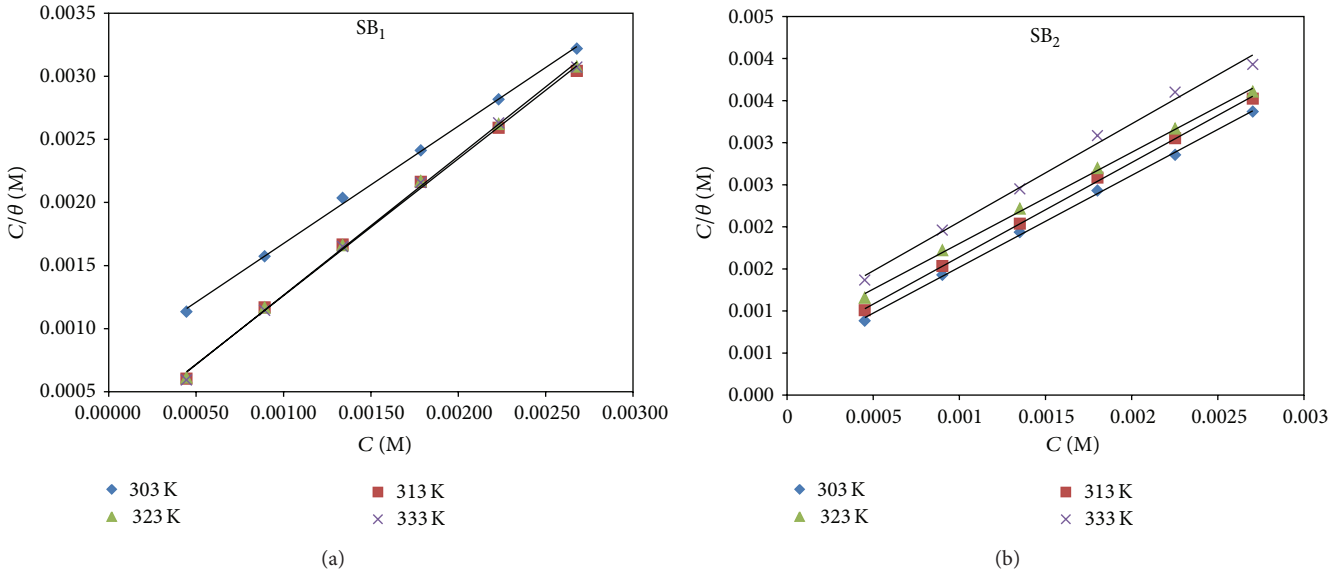

FIGURE 5: (a) Langmuir adsorption isotherm of SB_1 on mild steel in industrial medium at different temperatures. (b) Langmuir adsorption isotherm of SB_2 on mild steel in industrial medium at different temperatures.

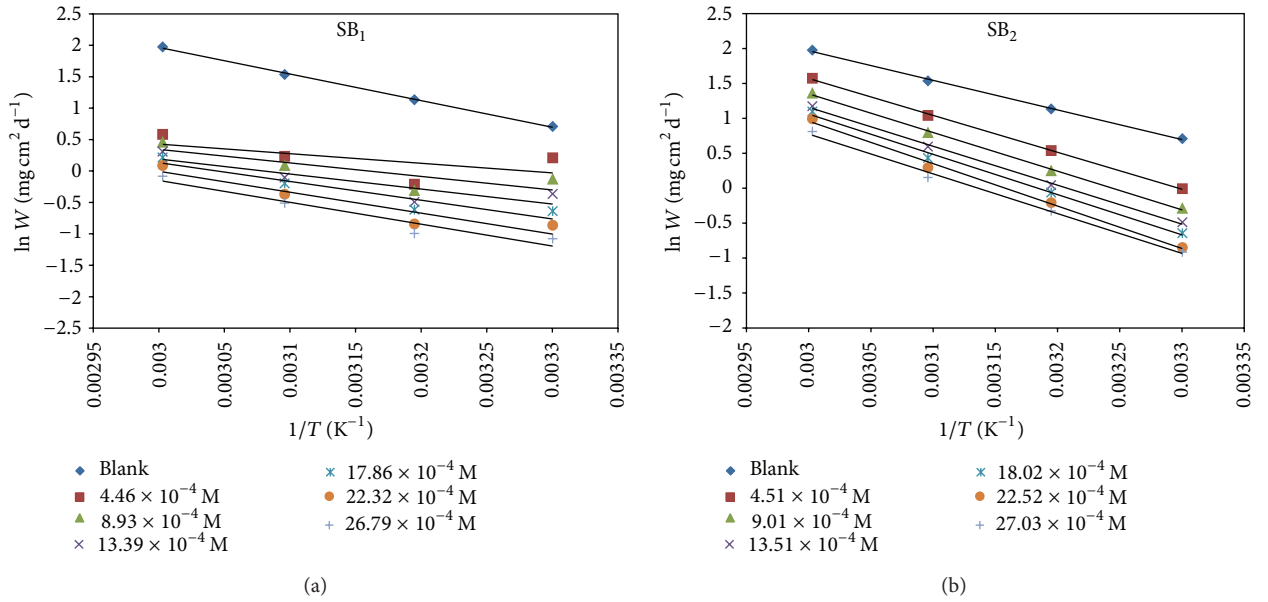

FIGURE 6: (a) Arrhenius plots of mild steel in industrial water medium in the absence and presence of different concentrations of SB_1. (b) Arrhenius plots of mild steel in industrial water medium in the absence and presence of different concentrations of SB_2.

where E_a^* is the activation energy, k is the preexponential constant, R is the universal gas constant, and T is the absolute temperature. Using (9), and from a plot of the log W versus $1/T$ (Figures 6(a) and 6(b)), the values of E_a^* and k at various concentrations of inhibitors were computed from slopes and intercepts, respectively, and the values are given in Table 4. The results in Table 4 show that the activation energy (E_a^*) for the corrosion of mild steel in the presence of the inhibitors is higher compared to the activation energy in the absence of inhibitor at all concentrations ranging from 4.46×10^{-4} M to 26.79×10^{-4} M. This can be attributed to the fact that higher values of E_a^* in the presence of inhibitors compared to its absence are generally consistent with a physisorption, while unchanged or lower values of E_a^* in inhibited solution suggest charge sharing or transfer from the organic inhibitor to the metal surface to form coordinate covalent bonds [41, 42]. The increase in E_a^* can be attributed to an appreciable decrease in the adsorption of the inhibitor on the steel surface with increase in temperature and a corresponding increase in corrosion rates occurs due to the fact that greater area of

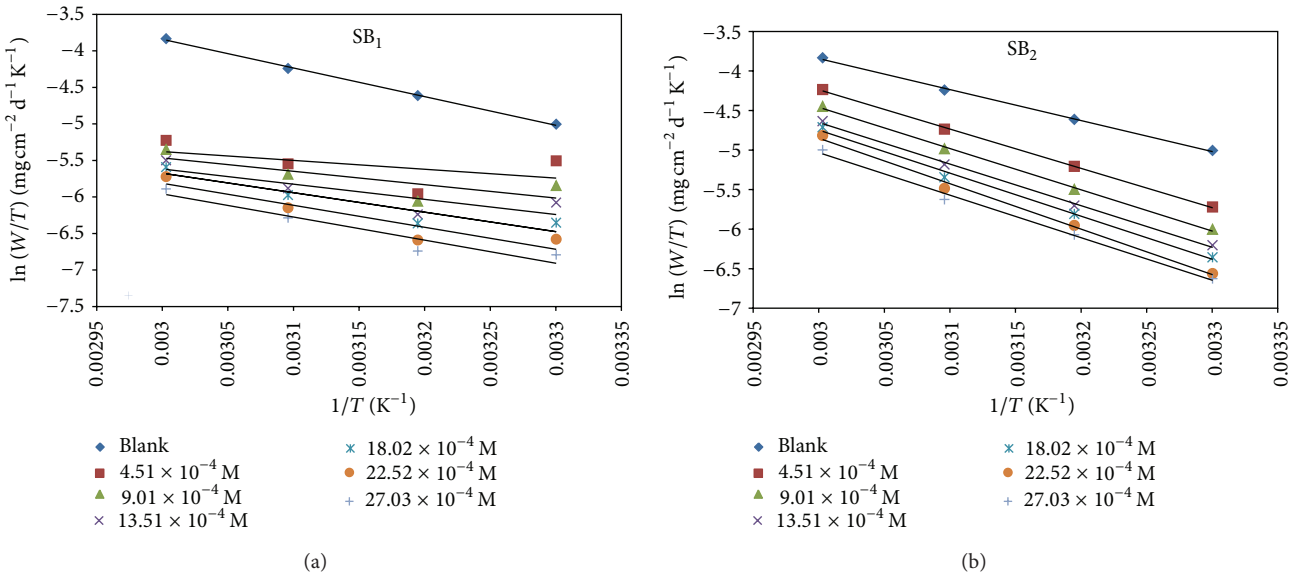

Figure 7: (a) Alternative Arrhenius plots of mild steel dissolution in industrial medium in the absence and presence of different concentrations of SB_1. (b) Alternative Arrhenius plots of mild steel dissolution in industrial medium in the absence and presence of different concentrations of SB_2.

Table 3: Adsorption parameters for adsorption of SB_1 and SB_2 on mild steel in industrial water medium at different temperatures from Langmuir adsorption isotherm.

Inhibitor	Temperature (K)	R^2	K_{ads} (L mol^{-1})	ΔG_{ads} (kJ mol^{-1})	ΔH_{ads} (kJ mol^{-1})	ΔS_{ads} (J mol^{-1} K^{-1})
SB_1	303	0.998	2500	−29.83	−21.90	−23.27
	313	0.999	2000	−30.23		
	323	0.998	1428	−30.29		
	323	0.998	1428	−30.29		
	333	0.993	1111	−30.54		
SB_2	303	0.998	1428	−28.42	−57.40	−11.15
	313	0.998	1428	−29.36		
	323	0.998	1111	−29.62		
	333	0.997	1000	−30.24		

Table 4: Activation parameters for mild steel in industrial water in the absence and presence of different concentrations of SB_1 and SB_2.

Inhibitor	Concentration (M)	K	E_a^* (kJ mol^{-1})	ΔH_a^* (kJ mol^{-1})	$\Delta H_a^* = E_a^* - RT$ (kJ mol^{-1})	ΔS_a^* (J mol^{-1} K^{-1})
SB_1	Blank	2378546	35.24	32.60	32.39	−131.69
	4.46×10^{-4}	7341105	39.39	36.75	36.53	−122.32
	8.93×10^{-4}	5797863	39.74	37.10	36.89	−124.29
	13.39×10^{-4}	7025099	40.93	38.29	38.07	−122.69
	17.86×10^{-4}	7873395	41.87	39.23	39.02	−121.73
	22.32×10^{-4}	12522029	43.64	41.00	40.79	−117.88
	26.79×10^{-4}	8268800	43.17	40.53	40.32	−121.33
SB_2	Blank	2378546	35.24	32.60	32.39	−131.69
	4.51×10^{-4}	37393221	43.97	41.33	41.12	−108.78
	9.01×10^{-4}	62582735	46.01	43.37	43.16	−104.50
	13.51×10^{-4}	59352215	46.39	43.75	43.54	−104.94
	18.02×10^{-4}	91972484	47.88	45.24	45.03	−101.29
	22.52×10^{-4}	211344487	50.47	47.83	47.61	−94.38
	27.03×10^{-4}	56288454	47.31	44.67	44.45	−105.38

Table 5: Quantum chemical parameters for SB_1 and SB_2.

Quantum parameters	SB_1				SB_2			
	PM3	AM1	RM1	MNDO	PM3	AM1	RM1	MNDO
E_{HOMO} (eV)	−8.99	−9.04	−9.03	−8.75	−8.15	−8.09	−8.04	−8.25
E_{LUMO} (eV)	−1.55	−1.39	−1.26	−1.21	−0.80	−0.38	−0.26	−0.49
ΔE (eV)	7.44	7.65	7.77	7.54	7.35	7.71	7.78	7.76
μ (Debye)	5.90	4.65	5.45	5.93	8.81	7.49	9.14	7.43

metal is exposed to solution [43]. The values of enthalpy and entropy of activation can be calculated from the alternative form of Arrhenius equation as follows:

$$W = \frac{RT}{Nh} \exp \frac{\Delta S_a^*}{R} \exp \frac{-\Delta H_a^*}{RT}, \quad (10)$$

where h is Planks constant, N is Avogadro's number, ΔS_a^* is the entropy of activation, and ΔH_a^* is the enthalpy of activation. A plot of $\log W/T$ versus $1/T$ should give straight lines (Figures 7(a) and 7(b)), with a slope of $(-\Delta H_a^*/2.303R)$, and an intercept of $[\log(RT/Nh)+(\Delta S_a^*/2.303R)]$, from which the values of ΔH_a^* and ΔS_a^* were calculated, respectively. The value of ΔH_a^* is reported in Table 4 and is positive. The positive sign of the enthalpy reflects the endothermic nature of carbon steel dissolution process. The increase in ΔH_a^* with increase in the concentration of the inhibitor for mild steel corrosion reveals that decrease in corrosion rate is mainly controlled by kinetic parameters of activation [44]. Also, the value of entropy of activation is negative. The negative value of entropy impies that the activated complex in the rate determining step represents an association rather than dissociation step, meaning that a decrease in disordering takes place on going from reactant to activated complex [45].

3.6. Quantum Chemical Study. Quantum chemical methods are useful in determining the molecular structure as well as elucidating the electronic structure and reactivity [46]. Therefore, it has become a common practice to carry out quantum chemical calculations in the field of corrosion inhibition studies. The selection of effective and appropriate inhibitors for the corrosion of metals has been widely carried out based on empirical approach [47, 48]. Computational methods are used to understand and explain the functions of organic compounds in molecular terms. In the present study, quantum chemical calculations were performed for investigating the relationship between the molecular structures of SB_1 and SB_2, and their inhibition effect on the mild steel surface. Table 5 presents the calculated values of semi-empirical parameters for SB_1 and SB_2 using PM3, AM1, RM1, and MNDO Hamiltonians. The calculated quantum chemical parameters included the energy of the highest occupied molecular orbital (E_{HOMO}) the energy of the lowest unoccupied molecular orbital (E_{LUMO}), and the energy gap (ΔE), the total energy of the molecule (TE) and the dipole moments (μ). These quantum chemical parameters are obtained after geometric optimization with respect to all nuclear coordinates.

The energy of HOMO (E_{HOMO}) is related to the electron donating ability of the molecule and high E_{HOMO} values indicate that the molecule has a tendency to donate orbital electrons to appropriate acceptor molecules with low energy or empty 3d orbital of Fe to form coordinate bond [49, 50]. Thus, increasing values of E_{HOMO} enable adsorption by influencing the transport process through the adsorbed layer. The energy of the LUMO (E_{LUMO}) indicates the ability of the molecule to accept electrons. The lower the value of E_{LUMO}, the more probable the molecule that would accept electrons, so that back-donating bond can be formed with its antibonding orbitals [51]. A good corrosion inhibitor is usually those organic compounds which not only offer electrons to unoccupied orbital of the metal, but also accept free electrons from the metal [52, 53]. Similarly, low values of the energy gap ($\Delta E = E_{LUMO} - E_{HOMO}$) yield good inhibition efficiencies, because the energy required to remove electron from the last occupied orbital will be low [49]. Low value of the dipole moment (μ) favours the accumulation of inhibitor molecules on the metallic surface [49]. In the present study the value of dipole moment of SB_1 is lower than that of SB_2. Thus, SB_1 is showing higher inhibition efficiency when compared to SB_2.

Figures 8(a)–8(c) and Figures 9(a)–9(c) show the HOMO density distribution, LUMO density distribution, and the Mulliken charge population analysis for SB_1 and SB_2 molecules. The use of Mulliken population analysis has been used to find out the adsorption centers of the inhibitors [54]. The higher negative charge of the adsorbed centre facilitates the atom to donate its electrons to the vacant 3d orbital of the metal [55, 56]. From Figures 8(c) and 9(c), it can be seen that N_7, N_8, N_{12}, S_{11}, O_{14}, O_{15}, C_4 in SB_1 and N_7, N_{10}, N_{11}, S_{14}, N_{15}, C_4 in SB_2 were the atoms with excess negative charges. Atoms N_{12} and N_{15} which have the highest negative charge, are adjacent to the carbon atom which is bonded with sulphur atom. This implies that the total electron density is located around these atoms. Therefore, the adsorption of SB_1 and SB_2 molecules on mild steel would take place through these atoms.

3.7. Scanning Electron Microscopy. Surface examination using SEM was carried out to study the effect of inhibitors on the surface morphology of mild steel. Figure 10(a) shows SEM image of a polished mild steel sample. Figure 10(b) shows SEM image of mild steel surface after immersion in industrial water without inhibitor for 10 h. This micrograph reveals that the surface was damaged in the absence of inhibitor. Figures 10(c) and 10(d) show SEM images of the surface of mild

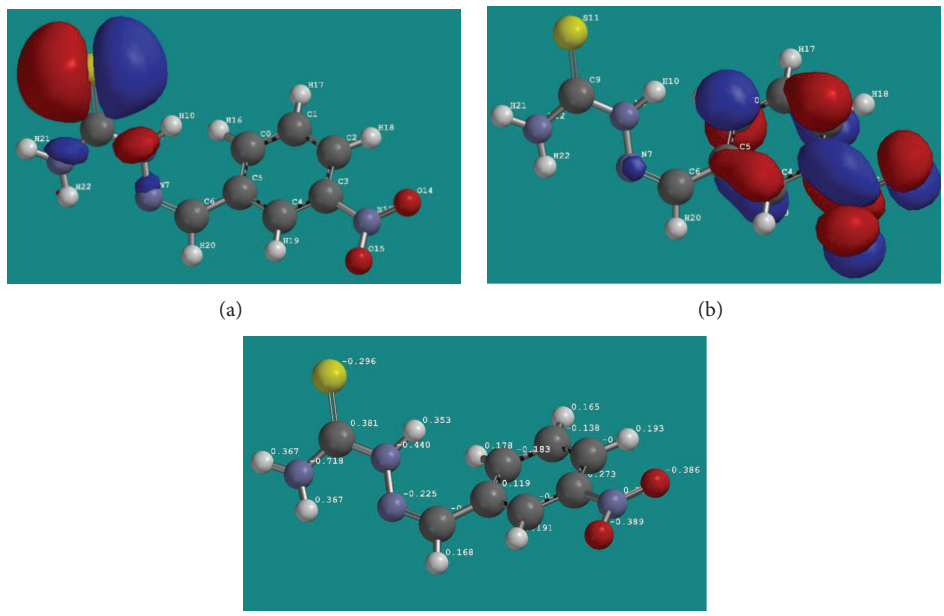

(a) (b)

(c)

Figure 8: (a) HOMO, (b) LUMO, and (c) the Mulliken charge density of the SB_1 molecule.

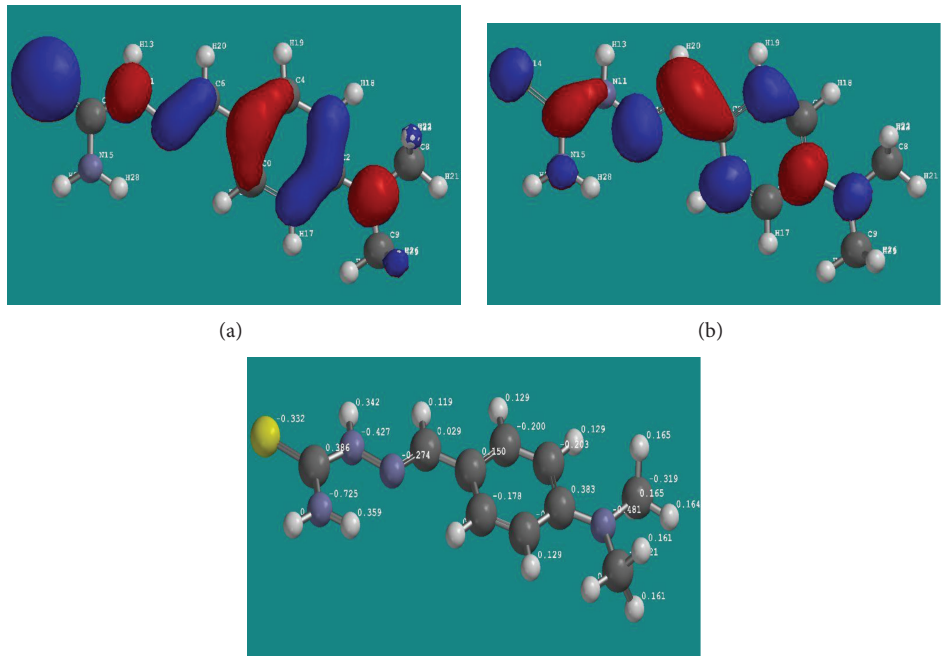

(a) (b)

(c)

Figure 9: (a) HOMO, (b) LUMO, and (c) the Mulliken charge density of the SB_2 molecule.

steel immersed for 10 h in industrial water containing 26.79×10^{-4} M and 27.03×10^{-4} M of SB_1 and SB_2, respectively. In Figures 10(c) and 10(d) the surface was free from pits and it was smooth. It can be concluded that the rate of corrosion is less in the presence of inhibitors. These observations also support the results of electrochemical studies and quantum chemical calculations pertaining to these inhibitors.

4. Conclusions

The Schiff bases (SB_1 and SB_2) used in the present study act as an efficient corrosion inhibitor for mild steel in industrial water. The maximum inhibition efficiencies of 88.07 and 80.23 were obtained from SB_1 and SB_2, respectively. The inhibition efficiency increases with the increase of inhibitor

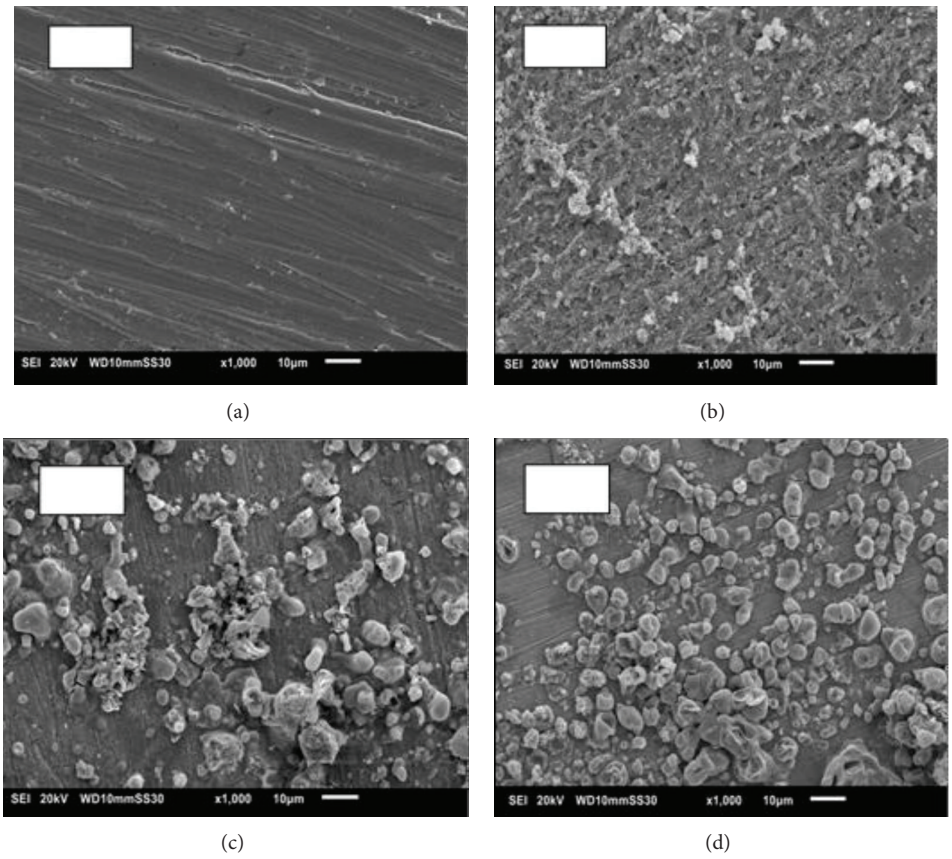

(a) (b)

(c) (d)

Figure 10: SEM images of mild steel in industrial water medium after 10 h immersion at 30°C. (a) Before immersion (polished), (b) without inhibitor, (c) with 26.79×10^{-4} M of SB_1, and (d) with 27.03×10^{-4} M of SB_2.

concentration and decreases with rising of temperature. The data obtained from all the studied techniques is in good agreement with each other. Both SB_1 and SB_2 behave as mixed type inhibitor and EIS results show that as the inhibitor concentration increases the charge transfer resistance also increases and the double layer capacitance decreases. Adsorption of both SB_1 and SB_2 on the mild steel surface in industrial water followed Langmuir adsorption isotherm. Quantum chemical parameters also proved that SB_1 and SB_2 act as an efficient inhibitor for the corrosion of mild steel in industrial water medium.

References

[1] S. S. Abd El-Rehim, S. A. M. Refaey, F. Taha, M. B. Saleh, and R. A. Ahmed, "Corrosion inhibition of mild steel in acidic medium using 2-amino thiophenol and 2-cyanomethyl benzothiazole," *Journal of Applied Electrochemistry*, vol. 31, no. 4, pp. 429–435, 2001.

[2] M. E. A. Abdullah, E. A. Helal, and A. S. Fouda, "Aminopyrimidine derivatives as inhibitors for corrosion of 1018 carbon steel in nitric acid solution," *Corrosion Science*, vol. 48, p. 1639, 2006.

[3] R. A. L. Sathiyanathan, S. Maruthamuthu, M. Selvanayagam, S. Mohanan, and N. Palaniswamy, "Corrosion inhibition of mild steel by ethanolic extracts of Ricinus communis leaves," *Indian Journal of Chemical Technology*, vol. 12, no. 3, pp. 356–360, 2005.

[4] I. L. Rozenfeld, *Corrosion Inhibitors*, McGraw-Hill, New York, NY, USA, 1981.

[5] A. Raman and P. Labine, *Reviews on Corrosion Inhibitor Science and Technology*, vol. 1, NACE, Houston, Tex, USA, 1986.

[6] M. Hosseini, S. F. L. Mertens, M. Ghorbani, and M. R. Arshadi, "Asymmetrical Schiff bases as inhibitors of mild steel corrosion in sulphuric acid media," *Materials Chemistry and Physics*, vol. 78, no. 3, pp. 800–808, 2003.

[7] A. K. Singh and M. A. Quraishi, "Effect of Cefazolin on the corrosion of mild steel in HCl solution," *Corrosion Science*, vol. 52, no. 1, pp. 152–160, 2010.

[8] G. K. Gomma, "Corrosion inhibition of steel by benzotriazole in sulphuric acid," *Materials Chemistry and Physics*, vol. 55, no. 3, pp. 235–240, 1998.

[9] A. M. Al-Mayout, A. K. Al-Amury, and A. A. Al-Suhybani, "Inhibition of type 304 stainless steel corrosion in 2 M sulfuric acid by some benzoazoles-time and temperature effects," *Corrosion*, vol. 57, no. 7, pp. 614–620, 2001.

[10] A. E. Stoyanova, E. I. Sokolova, and S. N. Raicheva, "The inhibition of mild steel corrosion in 1 M HCl in the presence of linear and cyclic thiocarbamides—effect of concentration and temperature of the corrosion medium on their protective action," *Corrosion Science*, vol. 39, no. 9, pp. 1595–1604, 1997.

[11] M. Abdallah, M. Al-Agez, and A. S. Fouda, "Phenylhydrazone derivatives as corrosion inhibitors for -α-brass in hydrochloric acid solutions," *International Journal of Electrochemical Science*, vol. 4, no. 3, pp. 336–352, 2009.

[12] X. J. Raj and N. Rajendran, "Corrosion inhibition effect of substituted thiadiazoles on brass," *International Journal of Electrochemical Science*, vol. 6, no. 2, pp. 348–366, 2011.

[13] M. Bouklah, N. Benchat, B. Hammouti, A. Aouniti, and S. Kertit, "Thermodynamic characterisation of steel corrosion and inhibitor adsorption of pyridazine compounds in 0.5 M H_2SO_4," *Materials Letters*, vol. 60, no. 15, pp. 1901–1905, 2006.

[14] S. C. Bell, G. L. Conklin, and S. J. Childress, "The separation of ketimine isomers," *Journal of the American Chemical Society*, vol. 85, no. 18, pp. 2868–2869, 1963.

[15] T. Mimani, S. M. Mayanna, and N. Munichandraiah, "Influence of additives on the electrodeposition of nickel from a Watts bath: a cyclic voltammetric study," *Journal of Applied Electrochemistry*, vol. 23, no. 4, pp. 339–345, 1993.

[16] W. Durnie, R. De Marco, A. Jefferson, and B. Kinsella, "Development of a structure-activity relationship for oil field corrosion inhibitors," *Journal of the Electrochemical Society*, vol. 146, no. 5, pp. 1751–1756, 1999.

[17] H. Shokry, M. Yuasa, M. Sekine, R. M. Isaa, H. Y. El Baradie, and G. K. Gomma, "Corrosion inhibition of mild steel by schiff base compounds in various aqueous solutions—part 1," *Corrosion Science*, vol. 40, no. 12, pp. 2173–2186, 1998.

[18] M. Hosseini, S. F. L. Mertens, M. Ghorbani, and M. R. Arshadi, "Asymmetrical Schiff bases as inhibitors of mild steel corrosion in sulphuric acid media," *Materials Chemistry and Physics*, vol. 78, no. 3, pp. 800–808, 2003.

[19] F. Baghaei, I. Sheikhshoaie, and A. Dadgarnezhad, "Investigation on some two bidentate N,O-Schiff base ligands as corrosion inhibitors on mild steel in sulfuric acid media," *Asian Journal of Chemistry*, vol. 17, no. 1, pp. 224–232, 2005.

[20] K. C. Emregul, R. Kurtaran, and O. Atakol, "An investigation of chloride-substituted Schiff bases as corrosion inhibitors for steel," *Corrosion Science*, vol. 45, no. 12, pp. 2803–2817, 2003.

[21] S. Deng, X. Li, and H. Fu, "Alizarin violet 3B as a novel corrosion inhibitor for steel in HCl, H_2SO_4 solutions," *Corrosion Science*, vol. 53, no. 11, pp. 3596–3602, 2011.

[22] S. S. A. El-Rehim, H. H. Hassan, and M. A. Amin, "The corrosion inhibition study of sodium dodecyl benzene sulphonate to aluminium and its alloys in 1.0 M HCl solution," *Materials Chemistry and Physics*, vol. 78, no. 2, pp. 337–348, 2002.

[23] A. Aytac, U. Ozmen, and M. Kabasakaloglu, "Investigation of some Schiff bases as acidic corrosion of alloy AA3102," *Materials Chemistry and Physics*, vol. 89, no. 1, pp. 176–181, 2005.

[24] S. L. Li, S. Chen, S. B. Lei, H. Ma, R. Yu, and D. Liu, "Investigation on some Schiff bases as HCl corrosioninhibitors for copper," *Corrosion Science*, vol. 41, no. 7, pp. 1273–1287, 1999.

[25] S. Chitra, K. Parameswari, and A. Selvaraj, "Dianiline schiff bases as inhibitors of mild steel corrosion in acid media," *International Journal of Electrochemical Science*, vol. 5, no. 11, pp. 1675–1697, 2010.

[26] S. Bilgic and N. Cabiskan, "An investigation of some Schiff bases as corrosion inhibitors for austenitic chromium-nickel steel in H_2SO_4," *Journal of Applied Electrochemistry*, vol. 31, no. 1, pp. 79–83, 2001.

[27] D. F. Shirver, P. W. Attinz, and C. H. Langford, *Inorganic Chemistry*, Oxford University Press, Oxford, UK, 2nd edition, 1994.

[28] S. Thota, S. S. Karki, K. N. Jayaveera, J. Balzarini, and E. D. Clercq, "Synthesis and cytotoxic activity of some mononuclear Ru(II) complexes," *Research Journal of Pharmaceutical, Biological and Chemical Sciences*, vol. 1, no. 3, pp. 704–713, 2010.

[29] P. T. Peter and S. T. C. Daniels, "Thiosemicarbazide as a reagent for the identification of aldehydes, ketones, and quinines," *Recueil des Travaux Chimiques*, vol. 69, pp. 1545–1547, 1958.

[30] M. Benabdellah, R. Touzani, A. Aouniti et al., "Inhibitive action of some bipyrazolic compounds on the corrosion of steel in 1 M HCl—part I: electrochemical study," *Materials Chemistry and Physics*, vol. 105, no. 2-3, pp. 373–379, 2007.

[31] P. Raja and M. Sethuraman, "Atropine sulphate as corrosion inhibitor for mild steel in sulphuric acid medium," *Materials Letters*, vol. 62, no. 10-11, pp. 1602–1604, 2008.

[32] H. Ashassi-Sorkhabi, M. R. Majidi, and K. Seyyedi, "Investigation of inhibition effect of some amino acids against steel corrosion in HCl solution," *Applied Surface Science*, vol. 225, no. 1–4, pp. 176–185, 2004.

[33] E. McCafferty and N. Hackerman, "Double layer capacitance of iron and corrosion inhibition with polymethylene diamines," *The Journal of The Electrochemical Society*, vol. 119, no. 2, pp. 146–154, 1972.

[34] E. E. Oguzie, Y. Li, and F. H. Wang, "Effect of 2-amino-3-mercaptopropanoic acid (cysteine) on the corrosion behaviour of low carbon steel in sulphuric acid," *Electrochimica Acta*, vol. 53, no. 2, pp. 909–914, 2007.

[35] J. M. Bastidas, J. L. Polo, and E. Cano, "Substitutional inhibition mechanism of mild steel hydrochloric acid corrosion by hexylamine and dodecylamine," *Journal of Applied Electrochemistry*, vol. 30, no. 10, pp. 1173–1177, 2000.

[36] E.-S. M. Sherif, R. M. Erasmus, and J. D. Comins, "Corrosion of copper in aerated acidic pickling solutions and its inhibition by 3-amino-1,2,4-triazole-5-thiol," *Journal of Colloid and Interface Science*, vol. 306, no. 1, pp. 96–104, 2007.

[37] J. Flis and T. Zakroczymski, "Impedance study of reinforcing steel in simulated pore solution with tannin," *Journal of the Electrochemical Society*, vol. 143, no. 8, pp. 2458–2464, 1996.

[38] F. Bentiss, M. Lebrini, and M. Lagrene, "Thermodynamic characterization of metal dissolution and inhibitor adsorption processes in mild steel/2,5-bis(*n*-thienyl)-1,3,4-thiadiazoles/hydrochloric acid system," *Corrosion Science*, vol. 47, no. 12, pp. 2915–2931, 2005.

[39] G. K. Gomma and M. H. Wahdan, "Schiffbases as corrosion inhibitors for aluminium in hydrochloric acid solution," *Materials Chemistry & Physics*, vol. 39, no. 3, pp. 209–213, 1995.

[40] M. R. Arshadi, M. Lashgari, and G. A. Parsafar, "Cluster approach to corrosion inhibition problems: interaction studies," *Materials Chemistry and Physics*, vol. 86, no. 2-3, pp. 311–314, 2004.

[41] A. Popova, M. Christov, and T. Deligeorgiev, "Influence of the molecular structure on the inhibitor properties of benzimidazole derivatives on mild steel corrosion in 1 M hydrochloric acid," *Corrosion*, vol. 59, no. 9, pp. 756–764, 2003.

[42] A. Popova, E. Sokolova, S. Raicheva, and M. Christov, "AC and DC study of the temperature effect on mild steel corrosion in acid media in the presence of benzimidazole derivatives," *Corrosion Science*, vol. 45, no. 1, pp. 33–58, 2003.

[43] I. B. Obot, N. O. Obi-Egbedi, and S. A. Umoren, "Antifungal drugs as corrosion inhibitors for aluminium in 0.1 M HCl," *Corrosion Science*, vol. 51, no. 8, pp. 1868–1875, 2009.

[44] T. Szauer and A. Brandt, "Adsorption of oleates of various amines on iron in acidic solution," *Electrochimica Acta*, vol. 26, no. 9, pp. 1253–1256, 1981.

[45] M. Bouklah, B. Hammouti, M. Lagrenée, and F. Bentiss, "Thermodynamic properties of 2,5-bis(4-methoxyphenyl)-1,3,4-oxadiazole as a corrosion inhibitor for mild steel in

normal sulfuric acid medium," *Corrosion Science*, vol. 48, no. 9, pp. 2831–2842, 2006.

[46] E. Kraka and D. Cremer, "Computer design of anticancer drugs. A new enediyne warhead," *Journal of the American Chemical Society*, vol. 122, no. 34, pp. 8245–8264, 2000.

[47] I. Lukovits, E. Kálmán, and F. Zucchi, "Corrosion inhibitors—correlation between electronic structure and efficiency," *Corrosion*, vol. 57, no. 1, pp. 3–8, 2001.

[48] I. Ahamad, R. Prasad, and M. A. Quraishi, "Adsorption and inhibitive properties of some new Mannich bases of Isatin derivatives on corrosion of mild steel in acidic media," *Corrosion Science*, vol. 52, no. 4, pp. 1472–1481, 2010.

[49] J. Fang and J. Li, "Quantum chemistry study on the relationship between molecular structure and corrosion inhibition efficiency of amides," *Journal of Molecular Structure: THEOCHEM*, vol. 593, no. 1–3, pp. 179–185, 2002.

[50] P. Zhao, Q. Liang, and Y. Li, "Electrochemical, SEM/EDS and quantum chemical study of phthalocyanines as corrosion inhibitors for mild steel in 1 mol/l HCl," *Applied Surface Science*, vol. 252, no. 5, pp. 1596–1607, 2005.

[51] D. Q. Zhang, Z. X. An, Q. Y. Pan, L. X. Gao, and G. D. Zhou, "Comparative study of bis-piperidiniummethyl-urea and mono-piperidiniummethyl-urea as volatile corrosion inhibitors for mild steel," *Corrosion Science*, vol. 48, no. 6, pp. 1437–1448, 2006.

[52] L. Lukovits, E. Kalman, and F. Zucchi, "Corrosion inhibitors—correlation between electronic structure and efficiency," *Corrosion*, vol. 57, no. 1, pp. 3–8, 2001.

[53] L. M. Rodrigues Valdez, W. Villamisar, M. Casales et al., "Computational simulations of the molecular structure and corrosion properties of amidoethyl, aminoethyl and hydroxyethyl imidazolines inhibitors," *Corrosion Science*, vol. 48, no. 12, pp. 4053–4064, 2006.

[54] N. K. Allam, "Thermodynamic and quantum chemistry characterization of theadsorption of triazole derivatives during Muntz corrosionin acidic and neutral solutions," *Applied Surface Science*, vol. 253, pp. 4570–4577, 2007.

[55] I. B. Obot and N. O. Obi-Egbedi, "Indeno-1-one [2,3-b]quinoxaline as an effective inhibitor for the corrosion of mild steel in 0.5 M H_2SO_4 solution," *Materials Chemistry and Physics*, vol. 122, no. 2-3, pp. 325–328, 2010.

[56] I. B. Obot, N. O. Obi-Egbedi, and S. A. Umoren, "The synergistic inhibitive effect and some quantum chemical parameters of 2,3-diaminonaphthalene and iodide ions on the hydrochloric acid corrosion of aluminium," *Corrosion Science*, vol. 51, no. 2, pp. 276–282, 2009.